Spin-dependent Andreev reflection tunneling through a quantum dot with intradot spin-flip scattering

Xiufeng Cao, Yaoming Shi *, Xiaolong Song and Shiping Zhou

Department of Physics, Shanghai University, Shanghai 200436, People's Republic of China

Hao Chen

Department of Physics, Fudan University, Shanghai 200433, People's Republic of China

Abstract

We study Andreev reflection (AR) tunneling through a quantum dot (QD) connected to a ferromagnet and a superconductor, in which the intradot spin-flip interaction is included. By using the nonequibrium-Green-function method, the formula of the linear AR conductance is derived at zero temperature. It is found that competition between the intradot spin-flip scattering and the tunneling coupling to the leads dominantes resonant behaviours of the AR conductance versus the gate voltage. A weak spin-flip scattering leads to a single peak resonance. However, with the spin-flip scattering strength increasing, the AR conductance will develop into a double peak resonannce implying a novel structure in the tunneling spectrum of the AR conductance. Besides, the effect of the spin-dependent tunneling couplings, the matching of Fermi velocity, and the spin polarization of the ferromagnet on the AR conductance is eximined in detail.

Key word: Spin-flip interaction, Andreev reflection, spin polarization

PACS numberm: 74.50.+r, 73.40.Gk, 72.25.Dc

1. Introduction

With the advances of nanofabrication and material growth technologies, it has been possible to realize various kinds of hybrid mesoscopic structures[1–4]. Recently, spin-dependent electronic transport through these hybrid mesoscopic structures has become one of the major focuses of the rapidly developing spintronics[5] for both its fundamental physics and potential applications. In particular, the Andreev reflection (AR) in spin-polarized transport through ferromagnet-superconductor (F-S) junctions has been examined based on the scattering matrix formulation[6–11]. It is found that in the case of low bias voltage, AR tunneling at the F-S interface is strongly affected by the spin polarization of the ferromagnet side[6] and the measuring of the differential AR conductance can successfully determine the spin polarization at the Fermi energy for several metals[7]. In addition, further calculations[8,9] showed that the AR conductance of F-S junction is also modified by the Fermi velocity mismatch, and it may even appear a peak with the varying of spin polarization of the ferromagnet.

On the other hand, spin-dependent resonant tunneling through a quantum dot (QD), a small system characterized by discrete electronic states, coupled a feeromagnet (F) and a superconductor (S) leads has been another interesting subject of experimental and theoretical investigations for the past decade. Zhu[12] et.al. proposed an efficient mechanism for the operation of writing spin in such the F-QD-S system with the principle of the Andreev reflection induced spin polarization. They[13] also studied the AR tunneling through a QD with two ferromagnets and a superconductor, in which only one spin-degenerate level of the QD is considered and the intradot Coulomb interaction is ignored. In this three terminal hybrid structure, the transport conducted by crossed AR, which involves an incident electron with spin σ from one of the ferromagnets picks up another electron with the opposed spin $\bar{\sigma}$ from the other one, both entre the S-lead and form a Cooper pair, is particularly interesting. It is found that the AR tunneling processes are, besides the spin polarizations and the matching condition of Fermi velocity, strongly dependent on the title angle between the magnetization orientations of the two F-leads. Feng and Xiong[14] investigated the transport properties of a F-QD-S system, in which both the Coulomb interaction and the multilevel structure of

the QD are considered. However, the spin-flip scattering is only included in the tunneling barriers.

Meanwhile, the significant role of spin-orbit interaction in the QD, which may cause the spin rotation of an electron while in the QD, has attracted considerable attentions more recently[15], especially in spin-polarized transport in magnetic nanostructures[16–19]. The spin-flip mechanisms in the GaAs-based QD have been investigated in Ref.[15]. Most of the theoretical studies[17–19] concentrate on exploring the effect of the intradot spin-flip scattering on linear and nonlinear conductances of F-QD-F systems in Kondo regime and a wide variety of novel features have been revealed. When the spin-flip scattering strength is of the order the Kondo temperature, the original single Kondo peak in the differential conductance is split into two peak or three peak structure due to the spin-flip process in the QD[18,19]. Hence, it is natural to ask if the intradot spin-flip scattering could induce some novel spectrum of tunneling AR conductance in the F-QD-S system.

In this paper we study the AR tunneling through a F-QD-S hybrid structure by using nonequlibrium Green Function method. We mainly emphasize the effect of the spin-flip scattering in the QD on linear AR conductance at zero temperature. Until now to our acknowledge, there are no theoretical research works to eximine this issue. The spin-flip scattering in the QD plays important roles for the AR process of such a F-QD-S system. For an isolated QD, it can split one spin-degenerate level of the QD, ε_d, to two spin-coherent levels, $\varepsilon_\pm = \varepsilon_d \pm R$, whose states are a superposition of the spin-up and spin-down ones. It implicates[17] that incident electrons with up-spin and down-spin from the left F-lead should tunnel coherently into the levels split by the intradot spin-flip scattering. In the spin-coherent tunneling process, it is expected for the Andreev reflection to bring about some novel resonant features of the conductance. We found that the competition between the level spliting and the broadening of the split levels arisen from the tunneling coupling, together with the spin polarization and the Fermi velocity matching condition, can determine the spin-up and spin-down populations of the QD, and further dominates resonant behaviors of

the AR conductance of the system. When the spin-flip scattering strength overbears that of the tunneling coupling to the leads, the AR conductance versus the gate voltage displays a symmetric double peak resonance, and the spin-flip scattering always suppresses the heights of the double peaks. However, for a weak spin-flip scattering process in the QD, it only leads to a single peak resonance of the AR conductance. In this case, as the spin-flip scattering strength increases, the height of the conductance peak may be first increased gradually and then dropped, depending the matching condition of the Fermi velocity.

.

2. The model and formulas

Consider resonant AR tunneling through a QD with the intradot spin-flip scattering connected to a F-lead and a S-lead, in which only one spin degenerate energy level is included and the Coulomb repulsion is ignored for simplicity. The spin quantization axis of the F-QD-S system is taken as the direction of the F-lead magnetization, along z-axis. The model is shown schematically in Fig.1. The Hamiltonian of the system under consideration, can be written as

$$H = H_F + H_S + H_{dot} + H_T \tag{1}$$

with

$$H_F = \sum_{k,\sigma} (\varepsilon_{k\sigma} + \sigma M) f^\dagger_{k\sigma} f_{k\sigma} \tag{2}$$

$$H_S = \sum_{p,\sigma} \varepsilon_{p\sigma} s^\dagger_{p\sigma} s_{p\sigma} + \sum_p (\Delta^* s^\dagger_{p\uparrow} s^\dagger_{-p\downarrow} + \Delta s_{p\uparrow} s_{-p\downarrow}) \tag{3}$$

$$H_{dot} = \sum_\sigma \varepsilon_d d^\dagger_\sigma d_\sigma + R(d^\dagger_\uparrow d_\downarrow + d^\dagger_\downarrow d_\uparrow) \tag{4}$$

$$H_T = \sum_{k,\sigma} (T_{k\sigma} f^\dagger_{k\sigma} d_\sigma + H.C.) + \sum_{p,\sigma} (T_{p\sigma} s^\dagger_{p\sigma} d_\sigma + H.C.) \tag{5}$$

where H_F and H_S are the Hamiltonians for the F-lead and the S-lead, respectively. Under mean-field approximation, the F-lead is characterized by a molecular magnetic moment $\vec{M}$.

The title angle between molecular magnetic moment and the F-QD interface is chosen to zero. The BCS Hamiltonian is adopted for the S-lead with an order parameter Δ standing for its energy gap. H_{dot} models the QD with single spin degenerate level ε_d. The spin-flip term in the H_{dot} is caused by spin-orbit interaction in the QD[15,17] and R is the spin-flip scattering strength. H_T describes the tunneling part between the QD and the F-lead and the S-lead with the tunneling matrixes $T_{k\sigma}$ and $T_{p\sigma}$. The spin conservation is assumed in the tunneling barrier processes, which is distinguished from that in Ref. [14].

The current flowing into the central region from the left ferromagnet lead can be evaluated from the time evaluation of the total electron number in the left lead[13,20]:

$$J_l = -e\langle\frac{dN_l(t)}{dt}\rangle = -\frac{e}{\hbar}\,\mathrm{Re}\sum_{k}^{i=1,3} T^{\dagger}_{k,l;ii}G^{<}_{k;ii}(t,t) \tag{6}$$

Here various kinds of Green functions are expressed in 4×4 Nambu representation[20]. The Green's functions of the electron of the QD can be exactly solved in the terms of Dyson's equation, $G^{r,a} = g^{r,a} + g^{r,a}\sum^{r,a} G^{r,a}$, in which $\sum^{r,a}$ is the self-energy due to both the spin-flip interaction in the QD and the spin-dependent tunneling couplings to the left and right leads, and $g^{r,a}$ is the Green function without both the tunneling coupling and the intradot spin-flip scattering:

$$(g^{r,a})^{-1} = \begin{pmatrix} \omega-\varepsilon_d \pm i0^+ & 0 & 0 & 0 \\ 0 & \omega+\varepsilon_d \pm i0^+ & 0 & 0 \\ 0 & 0 & \omega-\varepsilon_d \pm i0^+ & 0 \\ 0 & 0 & 0 & \omega+\varepsilon_d \pm i0^+ \end{pmatrix} \tag{7}$$

For the F-QD-S system studied, $\sum^{r,a}$ can be written as $\sum^{r,a} = \sum_R + \sum^{r,a}_{f\,0} + \sum^{r,a}_{s0}$. Here the off-diagonal term of H_{dot}, the intradot spin-flip scattering, is conveniently considered by the self-energy $\sum_R$:

$$\sum\nolimits_R = \begin{pmatrix} 0 & 0 & R & 0 \\ 0 & 0 & 0 & -R \\ R & 0 & 0 & 0 \\ 0 & -R & 0 & 0 \end{pmatrix} \tag{8}$$

The magnetization of the ferromagnet lead is described by introducing the spin polarization factor P. Then $\Gamma_{f\uparrow} = \Gamma_{f0}(1+P)$ and $\Gamma_{f\downarrow} = \Gamma_{f0}(1-P)$ stand for the spin-up and the spin-down tunneling coupling strengths to the F-lead, respectively, resulting in the spin-dependent linewidths of the QD level. $\Gamma_{f0} = 2\pi\rho_f^n T_k^* T_k$ is the spin-averaged coupling strength, $\Gamma_{f0} = \frac{1}{2}(\Gamma_{f\uparrow} + \Gamma_{f\downarrow})$ denoting the tunneling coupling between the QD and the F-lead without the internal magnetization. Within the wide bandwidth approximation, the self-energy coupling to the F-lead, $\sum_f^{r,a}$ is read as $\mp\frac{i}{2}\Gamma_f$. Here Γ_f can be written as:

$$\Gamma_f = \Gamma_{f0}\begin{pmatrix} (1+P) & 0 & 0 & 0 \\ 0 & (1-P) & 0 & 0 \\ 0 & 0 & (1-P) & 0 \\ 0 & 0 & 0 & (1+P) \end{pmatrix} \tag{9}$$

with P, the spin polarization in F-lead. The self-energy coupling to the S-lead is:

$$\Sigma_s^{r,a} = \mp\frac{i}{2}\rho_s^r(\omega)\Gamma_{s0}\begin{pmatrix} 1 & -\frac{\Delta}{\omega} & 0 & 0 \\ -\frac{\Delta}{\omega} & 1 & 0 & 0 \\ 0 & 0 & 1 & \frac{\Delta}{\omega} \\ 0 & 0 & \frac{\Delta}{\omega} & 1 \end{pmatrix} \tag{10}$$

where $\rho_s^r(\omega)$ is the dimensionless BCS density of states:

$$\rho_s^r(\omega) = \frac{|\omega|\,\theta(|\omega|-\Delta)}{\sqrt{\omega^2-\Delta^2}} + \frac{|\omega|\,\theta(\Delta-|\omega|)}{i\sqrt{\Delta^2-\omega^2}} \tag{11}$$

and $\Gamma_{s0} = 2\pi\rho_s^n T_p^* T_p$ is the tunneling coupling strength between the QD and the S-lead. ρ_s^n in Γ_{s0} is the normal density of state while the order parameter $\Delta = 0$. It is convenient to introduce the linewidth function matrices for the S-lead:

$$\Gamma_s = \rho_s^<(\omega)\Gamma_0\begin{pmatrix} 1 & -\frac{\Delta}{\omega} & 0 & 0 \\ -\frac{\Delta}{\omega} & 1 & 0 & 0 \\ 0 & 0 & 1 & \frac{\Delta}{\omega} \\ 0 & 0 & \frac{\Delta}{\omega} & 1 \end{pmatrix} \tag{12}$$

with $\rho_s^<(\omega) = |\omega|\,\theta(|\omega| - \Delta)/\sqrt{\omega^2 - \Delta^2}$. After a straightforward calculation, we obtain the formula of the tunneling current as follows:

$$J = J_N + J_A \tag{13}$$

with

$$J_N = \frac{e}{h}\int d\omega[f_l(\omega - eV) - f_r(\omega)] \sum_{i=1,3} [G_d^r \Gamma_s G_d^a \Gamma_f]_{ii} \tag{14}$$

and

$$J_A = \frac{e}{h}\int d\omega[f_l(\omega - eV) - f_l(\omega + eV)] \sum_{i=1,3}^{j=2,4} G_{d,ij}^r (\Gamma_f G_d^a \Gamma_f)_{ji} \tag{15}$$

where f_l and f_r are the Fermi-distribution functions in the left and right leads, respectively. J_N is the normal tunneling current which is caused by the single quasiparticle or quasihole transport, and J_A is the Andreev reflection current. In the linear response regime, the normal tunneling conductance and the AR conductance are obtained as follows::

$$G_N = \frac{e^2}{h}\int d\omega[-\frac{\partial f}{\partial \omega}] \sum_{i=1,3} [G_d^r \Gamma_s G_d^a \Gamma_f]_{ii} \tag{16}$$

and

$$G_A = \frac{2e^2}{h}\int d\omega[-\frac{\partial f}{\partial \omega}] \sum_{i=1,3}^{j=2,4} G_{d,\,i\,j}^r (\Gamma_f G_d^a \Gamma_f)_{ji} \tag{17}$$

Since the normal linear conductance is zero, $G_N = 0$, at zero temperature, only the Andreev reflection process contributes to the linear electronic transport of the system. So the total conductance G is equivalent to G_A.

3. The calculated results and discussion

We constrain ourselves only to discuss linear AR conductance at zero temperature for the F-QD-S, in which the energy level of the QD ε_d, controlled by the gate voltage V_g, is restricted in the range of the energy gap of the S-lead ($|\varepsilon_d| < \Delta$) and $|\varepsilon_d \pm R| < \Delta$. In the following calculation, both Fermi energies of the F- and S- leads are set to zero, the energy gap of the S- lead, Δ is taken as energy unit and the spin polarization is chosen as $P = 0.3$.

First we illustrate the effect of the intradot spin-flip scattering on resonant behaviors of the AR conductance versus the energy level of the QD, ε_d. In Fig.2, let $\Gamma_{s0} = 0.1$, we plotted the AR conductance as a function of ε_d in Fig.2(a) with $\Gamma_{f0} = 0.02$, Fig.2(b) $\Gamma_{f0} = 0.1$, and Fig.2(c) $\Gamma_{f0} = 0.2$, for some different spin-flip scattering strengths, $R = 0$ (solid line), 0.03 (dashed line), 0.05 (dotted line), 0.07 (dot-dashed line), 0.09 (dot-dot-dashed line), and 0.15 (short dashed line), respectively. In Fig.2(a), $\Gamma_{f0} < \Gamma_{s0}$, it is clearly seen that for a weak spin-flip scattering in the range of $R = 0 \sim 0.05$, the AR conductance displays a single peak resonance at the position of $\varepsilon_d = 0$ and its amplitude gradually rises till the maximum $G_m = 4e^2/h$, at $R_m \simeq \Gamma_{s0}/2 = 0.05$, with the R increasing. This is a perfect AR tunneling process. For some stronger spin-flip scatterings R ($0.05 \sim 0.06$), however, the AR conductance displays also a single peak profile at $\varepsilon_d = 0$, but the amplitude of the resonant peak reduces quickly. As the spin-flip scattering further increases, $R > 0.06$, the original single peak of the conductance develops to a well-resolved double peak resonance. The peaks appear near by $\pm R$, respectively. Furthermore, the intradot spin-flip scattering always suppresses the heights of the resonant bouble peaks.

Fig. 2(b) presents some curves of the resonant AR conductance for the symmetric tunneling couplings, $\Gamma_{f0} = \Gamma_{s0} = 0.1$, and other parameters are the same as those in Fig. 2(a). Comparing with Fig. 2(a), a strong enough spin-flip scattering R (> 0.08) brings about a double peak resonance of the conductance due to the larger broadening of two split levels $\Gamma = (2\Gamma_{f0} + \Gamma_{s0})$. It is found that the widths of the resonant double peaks enlarges for the enhanced broadening of the minority spin, $\Gamma_{f\downarrow}$. In Fig.2(c), $\Gamma_{f0} > \Gamma_{s0}$, the amplitude of the single peak resonance shows a novel feature: as the spin-flip scattering increases, the peak amplitude of the resonance is decreased monotonously. It is worth to notice that in the presence of the intradot spin-flip scattering, the single peak of the AR conductance exhibits characteristic behaviors essentially depending on a effective overlap of the broadening of the two split levels.

To elucidate the evolution of the resonant AR conductance from single peak to double peaks, we calculate the magnitude of the AR conductance at $\varepsilon_d = 0$, G_0, versus the spin-

flip scattering strength R. Defining the ratio of the two tunneling coupling strengths $r = \Gamma_{s0}/\Gamma_{f0}$, the matching condition of the Fermi velocity, $\Gamma_{f\uparrow} \cdot \Gamma_{f\downarrow} = \Gamma_{s0}^2$ reads now as $P^2 + r^2 = 1$. Fig. 3(a) shows some curves of the AR conductance G_0, for a given $\Gamma_{s0} = 0.1$ and several different $\Gamma_{f0} = 0.1$ (solid line), 0.1/3 (dashed line),0.1/5 (dotted line), 0.1/7 (dot-dashed line), 0.1/9 (dot-dot-dashed line). For the case of $r > 1$, the magnitude of G_0 increases firstly to its maximum $4e^2/h$ at R_m and then drops fastly as the spin-flip scattering strength R increases. It should be mentioned that for the $r > 1$ where the matching of the Fermi velocity can never been satisfied, G_0 should decrease monotonously with the spin polarization P increasing and can not reach to the maximum $4e^2/h$[13,14]. Our calculations indicated that there must exist, apart from what considered in Ref.[3] and [14], some other mechanisms that result in the perfect AR tunneling, G_0 rising to $4e^2/h$. We believe the intradot spin-flip scattering may account for it and leaving somewhat discussion in later. For a enough small Γ_{f0}, G_0 becomes a very sharp peak, and its maximum position R_m approaches very closely to $R = \Gamma_{s0}/2$. This means that if the spin-flip scattering strength slightly deviates from $\Gamma_{s0}/2$, the AR conductance quickly decreases from $4e^2/h$ to 0.

The typical feature showed in Fig.3(a) is understood qualitatively as follows. Spin-up and spin-down electrons can escape from the QD through the tunneling coupling to the leads, which leads to finite resonant broadening of the two spin-coherent split levels ($\varepsilon_d = \pm R$) by an amount Γ. Here $\Gamma = \Gamma_{s0} + \Gamma_{f\uparrow} + \Gamma_{f\downarrow} = (\Gamma_{s0} + 2\Gamma_{f0})$, the linewidth of the split levels, delineates the distribution of the density of states (DOS), in which $\Gamma_{f\uparrow}$ and $\Gamma_{f\downarrow}$ are spin-dependent tunneling rates to the F-side. Γ_{s0} is spin-independent tunneling rate to the S-side. When $R < R_m (\simeq \Gamma_{s0}/2)$, the linewidths of the two split levels are overlapped effectively at $\varepsilon_d = 0$, so that the AR conductance versus ε_d behaves as single peak resonance. In this situation, the AR conductance G_0, is enhanced with increasing R, because the intradot spin-flip scattering not only shift the level position of the QD from $\varepsilon_d = 0$ to $\varepsilon_d = \pm R$, but also change the spin-up and spin-down distribution of the DOS for the split levels[17]. Since the minority spin population near the Fermi energy determines behaviors of the AR tunneling, the spin-flip scattering turns effectively the majority spin carriers to minority

ones near $\varepsilon_d = 0$ resulting in G_0 to rises till its maximum $4e^2/h$, at R_m, in which spin-up and spin-down carriers from the F-lead completely form pairs into the S-lead. When $R > \Gamma_{s0}/2 + \Gamma_{f0} > R_m$, the two split levels have been shifted sufficiently away from each other leaving a vanishing spin-dependent DOS at $\varepsilon_d = 0$. Therefore G_0 drops quickly to zero and it should appear a deep valley in the resonant conductance curve. This implies that the AR conductance has developed into a well-resolved double peak resonance shown in Fig. 2(a). Fig. 3(b) presents the curves of the AR conductance, G_0 versus R with a fixed $\Gamma_{f0} = 0.1$ and several different Γ_{s0}, for $r > 1$. The peaks exist at a larger R_m than that in Fig. 3(a) owing to the stronger tunneling coupling rate Γ_{s0}, but their patterns are very analogous to each other due to the same spin minority $\Gamma_{f\downarrow}$.

In Fig.4(a), we plotted G_0 as a function of the spin-flip scattering strength R with a fixed $\Gamma_{s0} = 0.1$ and several different $\Gamma_{f0} = 0.1$ (solid line), 0.3 (dashed line),0.5 (dotted line), 0.7 (dot-dashed line), 0.9 (dot-dot-dashed line). This is the situation of $r < 1$, and the magnitude of G_0 decreases monotonously with R increasing. Since the linewidths $\Gamma_{f\uparrow}$ and $\Gamma_{f\downarrow}$ are much larger than Γ_{s0}, the spin-up and spin-down DOS are compatively low. With the increasing of spin-flip scattering, the minority spin occupation reduces gradually at $\varepsilon_d = 0$. Simultaneously, majority spin carriers can scarcely turn to minority ones near $\varepsilon_d = 0$ because of the requirement of the energy conversation. As a result, the magnitude of G_0 decreases monotonously with the R increasing. In Fig.4(b), we present some curvers of G_0 for the case of $r < 1$ with a fixed $\Gamma_{f0} = 0.1$, but for several different Γ_{s0}. Similar features, but a even faster drop of G_0 with R as in Fig.4(a), have been indicated. As is well-kown, Γ_{s0} describes the probability that two electrons in the QD tunnel into the S-lead and form a Cooper pair. So the weaker the Γ_{s0}, the less the probability, and the faster does the G_0 decrease to zero as the R increases.

4. Conclusion

In summary, we have studied the spin-dependent AR tunneling through a F-QD-S structure by using nonequilibrium Green function method. We found that the coherent spin-flip scattering in the QD plays important roles in the spin-dependent AR tunneling through the

F-QD-S system. The observed single or double peak resonant behaviors of the AR conductance, versus the gate voltage, is a consequence of the competition between the spin-flip scattering and the resonant broadenings of the two split levels due to the tunneling coupling to the leads. When the spin-flip scattering strength in the QD is smaller than the broadenings of the split levels, the AR conductance exhibites a single peak resonances. In this case, as the spin-flip scattering strength increases, the height of the single peak conductance may be first increased gradually and then deduced dropped quickly. However, when the spin-flip scattering induced spliting of the spin-degenerate level overbears the broadening of the split levels, the AR conductance appears as a symmetric double peak resonance, for which a novel structure in the tunneling spectrum of the AR conductance is predicted to appear. We expect the present results may have practical applications in the field of spintronics.

Acknowledgments: The authors are grateful to Qing-feng Sun for meaningful discussion and help. This work was supported by the National Natural Science Foundation of china (Grant No. 60371033) and by Shanghai Leading Academic Discipline Program, China. It was also supported by the Natural Science Foundation of China (NSFC) under Projects No.90206031, and the National Key Program of Basic Research Development of China(Grant No. G2000067107).

REFERENCES

* E-mail: ymshi@mail.shu.edu.cn

[1] W. Poirier, D. Mailly, and M. Sanquer, Phys. Rev. Lett. **79**. 2105 (1997)

[2] A. F. Morpurgo, B. J. Van Wees, T. M. Klapwijk, and G. Borghs, Phys. Rev. Lett. **79**, 4010 (1997).

[3] S. K. Upadhyay, A. Palanisami, R. N. Louie, and R. A. Buhrman, Phys. Rev. Lett. **81**, 3247 (1998).

[4] S. Gueron, M. M. Deshmmukh, E. B. Myers, and D. C. Ralph, Phys. Rev. Lett. **83**, 4148 (1999).

[5] G. Prinz, Science **282,** 1660 (1998); S. A. Wolf et al., Science **294**, 1488 (2001).

[6] M. J. M. de Jong and C. W. J. Beenakker, Phys. Rev. Lett. **74**, 1657 (1995).

[7] R. J. Soulen et al., Science **282**, 85 (1998).

[8] I. Žutić and A. D. Sarma, Phys. Rev. B **60**, R16322 (1999).

[9] I. Žutić and O. T. Valls, Phys. Rev. B **60**, 6320 (1999); **61** 1555(2000).

[10] R. Meseryvey and P. M. Tedrow, Phys. Rep. **238**, 173 (1994).

[11] G. E. Blonder, M. Tinkham, and T. M. Klapwijk, Phys. Rev. B **25**, 4515 (1982).

[12] Y. Zhu, Q. F. Sun and T. H. Lin, Phys. Rev. B **69**, 121302 (2004).

[13] Y. Zhu, Q. F. Sun and T. H. Lin, Phys. Rev. B **65**, 024516 (2001).

[14] A. F. Feng and S. J. Xiong, Phys. Rev. B **67**, 045316 (2003).

[15] A. V. Khaetskii and Y. V. Nazarov, Phys. Rev. B **61**, 12693 (2000); A. V. Khaetskii, Physica. **10E**, 27 (2001).

[16] W. Rudzinski and J. Barnaś, Phys. Rev. B **64**, 085318 (2001); F. M. Souza, J. C. Egues

and A. P. Jauho, cond-mat/0209263 (2002).

[17] P. Zhang, Q. K. Xue, Y. P. Wang, and X. C. Xie, Phys. Rev. Lett. **89**, 286803 (2002).

[18] R. López and D. Sánchez, Phys. Rev. Lett. **90**, 116602 (2003).

[19] J. Ma and X. L. Lei, cond-mat/0309520 (2003); B. Dong, H. L.Cai, S. Y. Liu, and X. L. Lei, J. Phys. Condes. Matter. **15**, 8435(2003).

[20] Z. Y. Zeng, F. Claro and Baowen Li, cond-mat/0110502 (2002).

FIGURES

Fig.1. The quantum dot with intradot spin-orbit interaction is coupled to a ferromagnet and a superconductor. A level of the QD is split into two spin coherent levels by the spin-flip interaction.

Fig.2. The resonant curves of the AR conductance versus the energy level of the QD, ε_d, with parameters $P = 0.3$, $\Gamma_{s0} = 0.1$ and several spin-flip scattering strengths $R = 0$ (solid line), 0.03 (dashed line), 0.05 (dotted line), 0.07 (dot-dashed line), 0.09 (dot-dot-dashed line), and 0.15 (short dashed line) for three different spin-averaged tunneling couplings to the F-lead: (a) $\Gamma_{f0} = 0.02$, $\Gamma_{f0} < \Gamma_{s0}$, (b) $\Gamma_{f0} = 0.1$, $\Gamma_{f0} = \Gamma_{s0}$, and $\Gamma_{f0} = 0.2$, $\Gamma_{f0} > \Gamma_{s0}$.

Fig.3. The AR conductance at $\varepsilon_d = 0$, G_0 versus the R with a parameter $P = 0.3$ (a). $\Gamma_{f0} < \Gamma_{s0}$ and $\Gamma_{s0} = 0.1$, the curves of the conductance for some different $\Gamma_{f0} = 0.1$ (solid line), 0.1/3 (dashed line), 0.1/5 (dotted line), 0.1/7 (dot-dashed line), 0.1/9 (dot-dot-dashed line). (b). $\Gamma_{f0} < \Gamma_{s0}$ and $\Gamma_{f0} = 0.1$, the curves of the conductance for $\Gamma_{s0} = 0.1$ (solid line), 0.3 (dashed line), 0.5 (dotted line), 0.7 (dot-dashed line), 0.9 (dot-dot-dashed line).

Fig.4 The G_0 versus R with a parameter $P = 0.3$, $\Gamma_{f0} > \Gamma_{s0}$ (a). $\Gamma_{s0} = 0.1$, the curves of the conductance for some different $\Gamma_{f0} = 0.1$ (solid line), 0.3 (dashed line), 0.5 (dotted line), 0.7 (dot-dashed line), 0.9 (dot-dot-dashed line). (b). $\Gamma_{f0} = 0.1$, the curves of the conductance for $\Gamma_{s0} = 0.1$ (solid line), 0.1/3 (dashed line), 0.1/5 (dotted line), 0.1/7 (dot-dashed line), 0.1/9 (dot-dot-dashed line).

Fig. 1

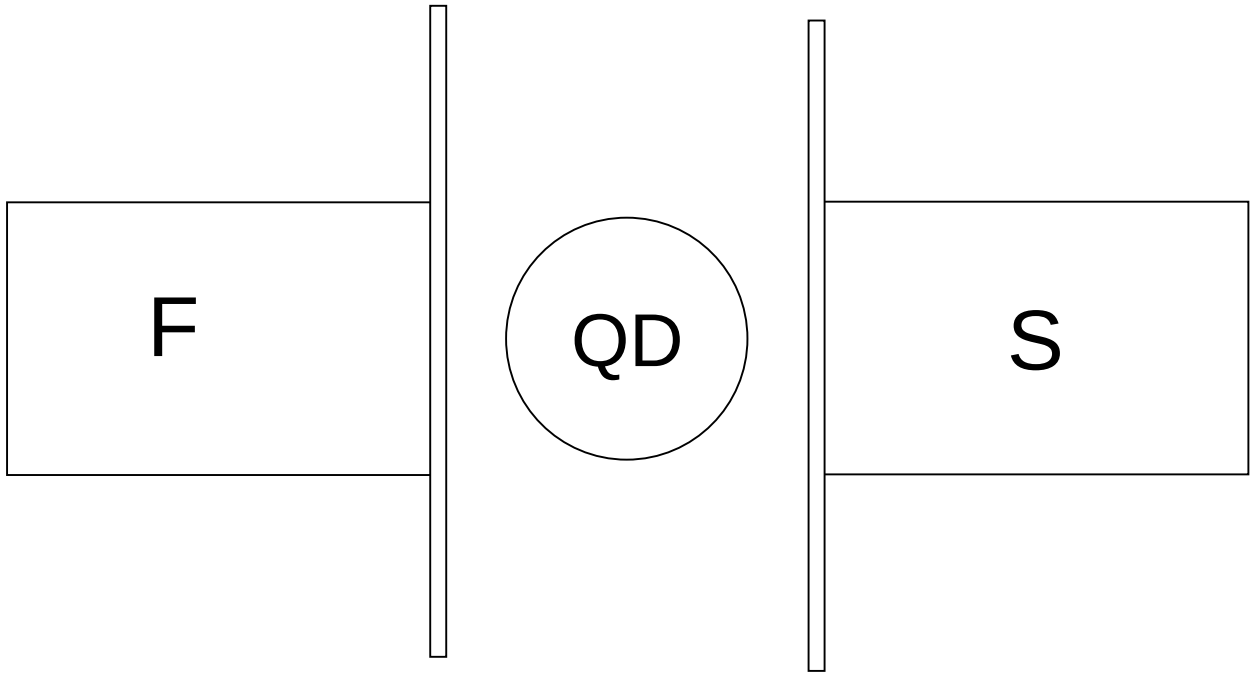

Fig. 2

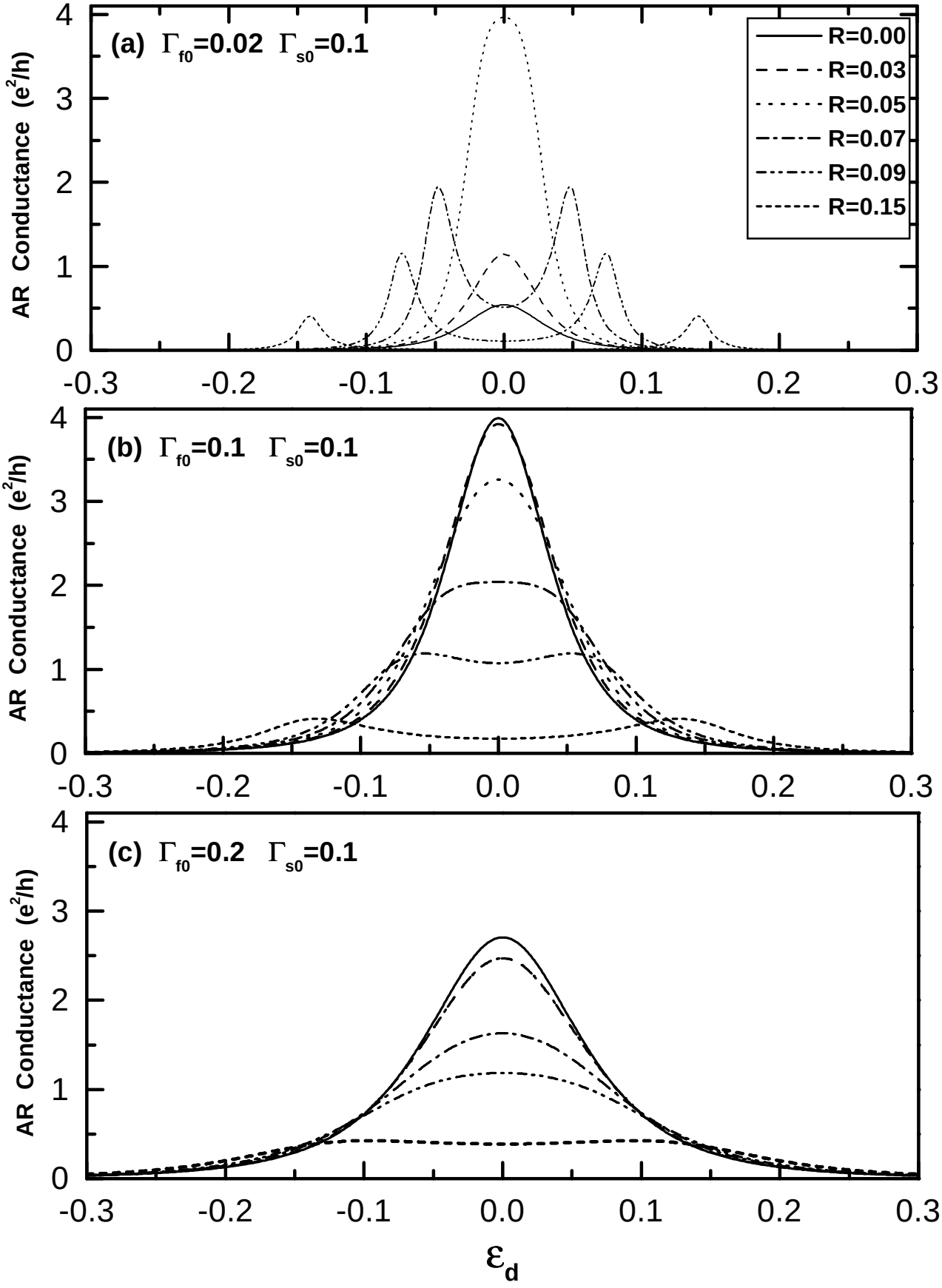
(a) Γf0=0.02 Γs0=0.1
R=0.00
R=0.03
R=0.05
R=0.07
R=0.09
R=0.15
AR Conductance (e²/h)
(b) Γf0=0.1 Γs0=0.1
AR Conductance (e²/h)
(c) Γf0=0.2 Γs0=0.1
AR Conductance (e²/h)
0
1
2
3
4
-0.3
-0.2
-0.1
0.0
0.1
0.2
0.3
εd

Fig. 3

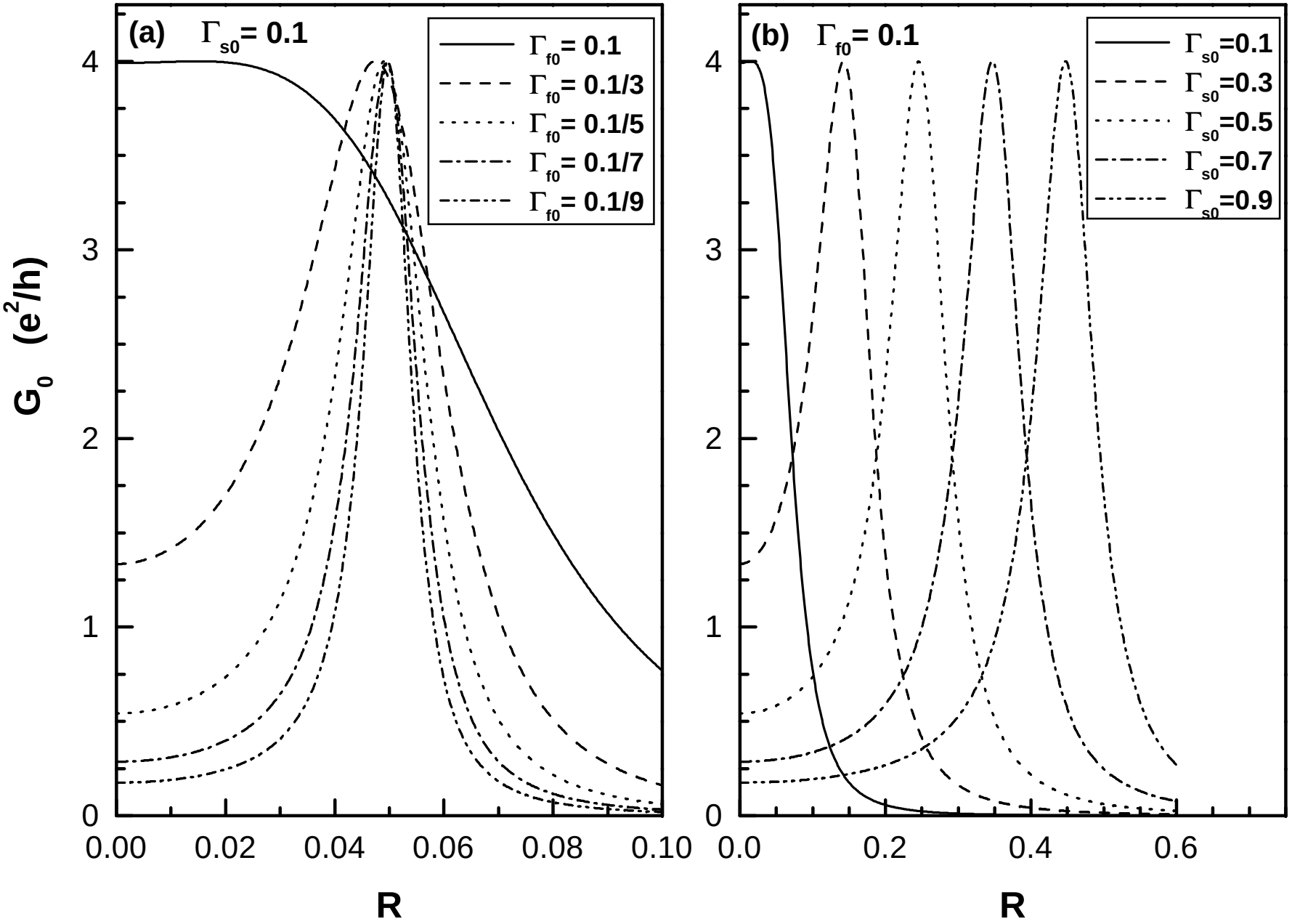
(a) Γ_{s0}= 0.1
Γ_{f0}= 0.1
Γ_{f0}= 0.1/3
Γ_{f0}= 0.1/5
Γ_{f0}= 0.1/7
Γ_{f0}= 0.1/9
G_0 (e^2/h)
R
(b) Γ_{f0}= 0.1
Γ_{s0}=0.1
Γ_{s0}=0.3
Γ_{s0}=0.5
Γ_{s0}=0.7
Γ_{s0}=0.9
R

Fig. 4

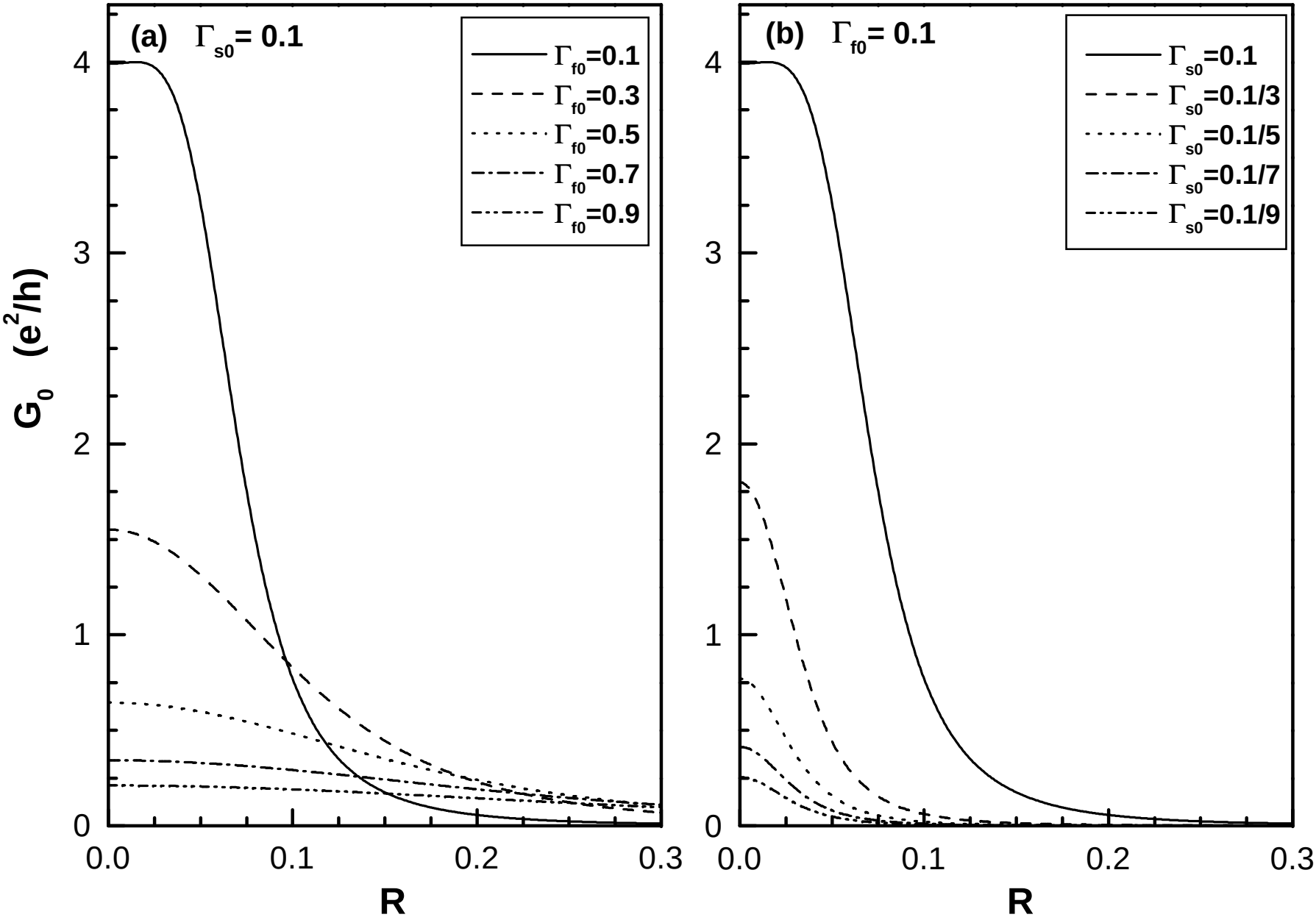
(a) Γ_{s0}= 0.1
Γ_{f0}=0.1
Γ_{f0}=0.3
Γ_{f0}=0.5
Γ_{f0}=0.7
Γ_{f0}=0.9
G_0 (e^2/h)
R
(b) Γ_{f0}= 0.1
Γ_{s0}=0.1
Γ_{s0}=0.1/3
Γ_{s0}=0.1/5
Γ_{s0}=0.1/7
Γ_{s0}=0.1/9
R